Int. J. Heat Mass Transfer. Vol. 17, pp. 933–943. Pergamon Press 1974. Printed in Great Britain

ENHANCEMENT OF CONDENSATION HEAT TRANSFER IN THE PRESENCE OF NONCONDENSABLE BY VISCOUS DISSIPATION

M. SADDY† and F. V. DEL POZO
Programa de Engenharia Quimica, COPPE/UFRJ, Caixa Postal 1191 Rio de Janeiro, Brazil

(*Received* 15 *March* 1973)

Abstract—A simple model based on forced convection condensation boundary-layer flow is proposed to study the mechanisms by which heat is transferred to a solid wall, in the presence of noncondensable and superheating, plus viscous dissipation in the gas–vapour side.

The results are numerically obtained for the specific system consisting of steam and air, at a saturation temperature of 212°F and several degrees of superheating and noncondensable mass fractions of practical applications.

It is demonstrated that through an increase in the temperature at the condensate-gas–vapour interface, the effect of viscous dissipation is to decrease the thickness of the thermal boundary-layer set up on the vapour side on top of the condensate, in a similar manner as the effect caused by superheating. Both effects cause an increase in the heat flux to the wall.

NOMENCLATURE

C_p, specific heat at constant pressure;
D, binary diffusion coefficient;
Ec, Eckert number, $= U^2/C_p(T_\infty - T_i)$;
f, dimensionless stream function, equation (1a);
g, dimensionless stream function, equation (1b);
h_{fg}, latent heat of condensation;
k, thermal conductivity;
L, characteristic length in Re;
M, molecular weight;
p, partial pressure;
P, total pressure;
Pr, Prandtl number, $= \nu/\alpha$;
$\overline{Pr}$, temperature averaged Prandtl number;
q, surface heat flux;
R, property ratio, $[(\rho\mu)_L/(\rho\mu)]^{1/2}$;
Re, Reynolds number, $= UL/\nu$;
Sc, Schmidt number, $= \nu/D$;
T, temperature;
u, v, velocity components;
U, free stream velocity;
W, mass fraction of noncondensable;
x, y, coordinates.

Greek symbols

α, thermal diffusivity, $= k/\rho C_p$;
δ, condensate layer thickness;
η, similarity variable, equation (1a);
η_δ, value of η at $y = \delta$;
Θ, dimensionless temperature, $(T - T_\infty)/(T_i - T_\infty)$;
θ, dimensionless temperature, $(T - T_w)/(T_i - T_w)$;
μ, absolute viscosity;
ν, kinematic viscosity;
ξ, similarity variable, equation (1b);
ξ_d, value of ξ at the edge of the concentration boundary-layer;
ξ_T, value of ξ at the edge of the thermal boundary-layer;
ξ_V, value of ξ at the edge of the velocity boundary-layer in the vapour side;
ρ, density;
ψ, Ψ, stream functions;
φ, mass fraction variable, $W_g - W_{g\infty}$.

Subscripts

L, condensate;
V, vapour;
g, gas;
i, interface;
w, solid surface;
∞, free stream;
sat, ∞, saturation at free stream.

Superscripts

$'$, first derivative;
$''$, second derivative;
$*$, saturated vapour;
$**$, superheated vapour in the absence of viscous dissipation.

†Associate Professor.

INTRODUCTION

THE THEORETICAL study of condensation heat transfer in forced convection boundary-layer flows consisting of a pure vapour or a mixture of a vapour with non-condensable gases has been extensively dealt with in the current literature. The mechanism by which heat is conducted through the layer of condensate to the solid wall, as transferred from the vapour–gas main stream is well understood.

The effect of vapour superheating is known to enhance the heat flux to the wall mainly in the presence of noncondensables [1], whereas small amounts of non-condensables in a saturated vapour stream work in the opposite direction [2]. In both cases the effective thermal driving force between the interface and the wall is substantially diminished due to the accumulation of the noncondensable at the impermeable interface, which reduces the vapour pressure and the temperature there. In the former situation, however, heat is also conducted from the free stream through the vapour layer to the interface, hence contributing to raise the interface temperature slightly. Thus, increasing the effective thermal driving force.

It may be anticipated now that the role the viscous dissipation, in the superheated free stream, is expected to play is also in the direction of increasing the interfacial temperature thereby enhancing the heat flux to the solid plate. The question raised in this work is how pronounced that effect is and in what circumstances.

The formulation of the problem is based on forced convection boundary-layer theory. The model consists of a thin liquid layer of condensate in contact with the solid flat plate on top of which the vapour–gas mixture flows. Momentum and thermal boundary-layers will form in the vapour phase, with the interface kept at the saturation state. The schematic diagram of this physical picture is shown in the Fig. 1.

The results for heat transfer are obtained in a simplified but accurate manner from an integral solution of the governing equations, using the method due to Kármán–Pohlhausen. Wide range of vapour superheat, stream-to-wall temperature difference, Eckert number and a saturation temperature of 212°F have been used in the numerical computations.

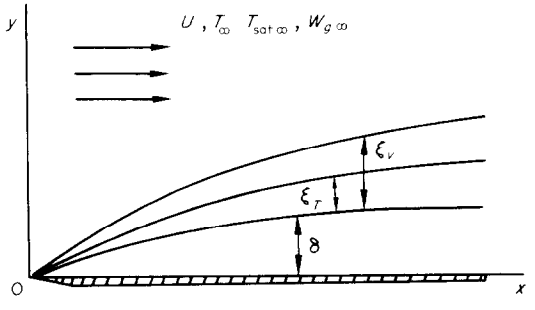

FIG. 1. Schematic diagram and coordinate system.

ANALYSIS AND SOLUTION

The presentation of the problem in analytical terms will be concise for most of it has been published in the literature [2]. Thus liberal references will be made to their analysis with the modifications appropriate to the inclusion of the viscous dissipation term.

The velocity boundary-layers

When similarity transformations such as

$$\eta = y\sqrt{\frac{U}{v_L x}}, \quad 0 \leqslant y \leqslant \delta$$

$$\psi = \sqrt{v_L U x}\, f(\eta) \tag{1a}$$

and

$$\xi = (y-\delta)\sqrt{\frac{U}{vx}}, \quad y \geqslant \delta$$

$$\Psi = \sqrt{vUx}\, g(\xi) \tag{1b}$$

for the liquid condensate and vapour–gas boundary-layers, respectively, are introduced in the momentum and continuity equations, the following velocity fields result. For the liquid side the solution is readily obtained:

$$f'(\eta) = \frac{u}{U} = f'(\eta_\delta)\frac{\eta}{\eta_\delta} \tag{2}$$

and

$$f(\eta) = f'(\eta_\delta)\frac{\eta^2}{2\eta_\delta}. \tag{3}$$

For the vapour side a solution is assumed which has the following form:

$$g'(\xi) = \frac{u}{U} = \left\{f'(\eta_\delta) + 2\frac{\xi}{\xi_V} - \left(\frac{\xi}{\xi_V}\right)^2\right\}. \tag{4}$$

When the above profile is introduced into the momentum equation, it results after some manipulation:

$$2g''(0) = g(0)[1-g'(0)] + \int_0^{\xi_T} g'(\xi)\,\mathrm{d}\xi - \int_0^{\xi_V} [g'(\xi)]^2\,\mathrm{d}\xi$$

or

$$\tfrac{1}{5}\xi_V^2\left[\tfrac{2}{3} + f'(\eta_\delta)\right] + g(0)\xi_V - 4 = 0. \tag{5}$$

In the above equations the condition is satisfied that the liquid velocity at the interface, as given by $f'(\eta_\delta)$, is negligibly small, as evidenced in [3–5].

The temperature boundary-layers

The solution to the energy equation in the condensate layer is reduced to a linear form, by neglecting the second order convective terms, as usual:

$$\theta(\eta) = \frac{T(\eta) - T_w}{T_i - T_w} = \frac{\eta}{\eta_\delta}. \tag{6}$$

For the vapour–gas region the complete energy equation is considered, with the viscous dissipation term included:

$$u\frac{\partial T}{\partial x} + v\frac{\partial T}{\partial y} = \alpha\frac{\partial^2 T}{\partial y^2} + \frac{\mu}{\rho C_p}\left(\frac{\partial u}{\partial y}\right)^2 \tag{7}$$

which becomes after application of the similarity transformation (1b)

$$\Theta''(\xi) + \tfrac{1}{2} Pr\, g(\xi)\Theta'(\xi) = Ec\, Pr[g''(\xi)]^2, \qquad 0 \leqslant \xi \leqslant \xi_T \tag{8}$$

where the r.h.s. is the term which accounts for the conversion of the kinetic energy of the motion into heat. In equation (8), $Ec = U^2/C_p(T_\infty - T_i)$, $\Theta(\xi) = (T(\xi) - T_\infty)/(T_i - T_\infty)$, and $Pr = \mu C_p/k$ is the gas–vapour mixture Prandtl number.

Its solution, assumed to be of a parabolic type,

$$\Theta(\xi) = 1 - 2\frac{\xi}{\xi_T} + \frac{\xi^2}{\xi_T^2}, \quad \text{with} \quad \left\{-\Theta'(0)\right\} = \frac{2}{\xi_T} \tag{9}$$

is introduced into the energy equation to produce the following expression in its integral form, assuming Ec and $\overline{Pr}$ constants:

$$\frac{2}{Pr}\Theta'(0) + g(0) + \int_0^{\xi_T} g'(\xi)\Theta(\xi)\,d\xi = -2Ec\int_0^{\xi_T}\{g''(\xi)\}^2\,d\xi. \tag{10}$$

Now, consideration must be given as to whether ξ_V is greater or less than ξ_T, so that equation (10) could be integrated for the velocity profile given by equation (4):

$$\left\{\frac{80Ec}{\xi_V^2} - 1\right\}\frac{\xi_T^4}{30\xi_V^2} - \left\{\frac{48Ec}{\xi_V^2} - 1\right\}\frac{\xi_T^3}{6\xi_V} + \left\{\frac{24Ec}{\xi_V^2} + f'(\eta_\delta)\right\}\frac{\xi_T^2}{3} + g(0)\xi_T - \frac{4}{\overline{Pr}} = 0, \qquad \text{for} \quad \xi_V > \xi_T \tag{11}$$

and

$$\left(\frac{8Ec}{3\xi_V^4}\right)\xi_T^5 - \left(\frac{8Ec}{\xi_V^3}\right)\xi_T^4 + \left\{\frac{24Ec}{\xi_V^2} + 1\right\}\frac{\xi_T^3}{3} + \left\{g(0) - \frac{\xi_V}{3}\right\}\xi_T^2 + \left\{\frac{\xi_V^2}{6} - \frac{4}{\overline{Pr}}\right\}\xi_T - \frac{\xi_V^3}{30} = 0, \qquad \text{for} \quad \xi_V < \xi_T. \tag{12}$$

The actual value of $\overline{Pr}$, which is an average between those at temperatures $T_{sat,\infty}$ and T_i, will determine which equation to use, either equation (11) or (12), depending essentially upon the values of Pr at T_i.

The concentration boundary-layer

The diffusion boundary-layer equation is applied to the model

$$\varphi''(\xi) + \tfrac{1}{2} Sc\, g(\xi)\varphi'(\xi) = 0 \tag{13}$$

with $\varphi(\xi) = W_g - W_{g\infty}$ as the difference between the gas mass fractions at any point within the layer and its value outside it in the free stream. The following relationships hold:

$$W_V + W_g = 1 \qquad W_g = \frac{\rho_g}{\rho}$$

and

$$\rho_V + \rho_g = \rho \qquad W_V = \frac{\rho_V}{\rho}.$$

The assumption that Sc is constant and less than unity for the system and in the range of temperatures to be used in this work, makes it possible to integrate equation (13), after replacing the profile for $\varphi(\xi)$:

$$\varphi(\xi) = \varphi(0)\left[1 - 2\frac{\xi}{\xi_d} + \left(\frac{\xi}{\xi_d}\right)^2\right] \tag{14}$$

$$[-\varphi'(0)] = 2\frac{\varphi(0)}{\xi_d}$$

resulting for values of $\xi_d > \xi_V$:

$$\xi_d^3 + [3g(0) - \xi_V]\xi_d^2 + \left[\frac{1}{2}\xi_V^2 - \frac{12}{Sc}\right]\xi_d - \frac{1}{10}\xi_V^3 = 0. \tag{15}$$

In this equation use has been made of condition e at the interface described below.

The interface condensate-gas–vapour mixture

That interface is defined by either of the following coordinates

$$y = \delta, \quad \eta = \eta_\delta \quad \text{or} \quad \xi = 0.$$

All the expressions for continuities at the interface listed below have been derived in the second paper mentioned in the introduction to this work:

a, streamwise velocity component, $f'(\eta_\delta) = g'(0)$;

b, shear stress, $Rf''(\eta_\delta) = g''(0)$;

c, mass across the interface, $Rf(\eta_\delta) = g(0)$;

d, temperature, $\theta(\eta_\delta) = \Theta(0) = 1$;

e, impermeability to the noncondensable,

$$\frac{\varphi'(0)}{\varphi(0) + W_{g\infty}} = -\tfrac{1}{2} Sc\, g(0);$$

f, energy across the interface,

$$\tfrac{1}{2}g(0) + [-\Theta'(0)]\frac{C_p(T_\infty - T_i)}{Pr\, h_{fg}} = \theta'(\eta_\delta)\frac{R\,C_{p_L}}{Pr_L h_{fg}}(T_i - T_w).$$

In all the six conditions above the figures for the physical and transport properties are taken at T_i.

Finally, if the perfect gas law holds good, the saturation vapour partial pressure is related to the gas mass fraction and the system total pressure by:

$$\frac{p_V}{P} = \frac{1-W_g}{1-W_g\left(1-\frac{M_V}{M_g}\right)}. \tag{16}$$

In the above expression if $W_g = W_{g\infty}$, p_V is that corresponding to $T_{\text{sat},\infty}$. On the other hand if T_i is known, p_{Vi} is found from the saturation state data and W_{gi} can be calculated.

Method of computation

In the description of the formulation of the problem up to this point, it has been clear that the solution to the set of algebraic equations involves nine unknowns ($f'(\eta_\delta)$, ξ_V, η_δ, $g(0)$, ξ_d, ξ_T, W_{gi}, P and T_w) and eight parameters (R, $W_{g\infty}$, Pr, Pr_L, Ec, Sc, $T_\infty - T_{\text{sat},\infty}$ and $T_{\text{sat},\infty}$). Once the problem is specified to a particular system of fluids, it is reasonable to regard Sc, $T_{\text{sat},\infty}$, $T_\infty - T_{\text{sat},\infty}$ and $W_{g\infty}$ as known quantities. Moreover, three out of the remaining four parameters depend only on the value of T_i: R, Pr_L, Pr. The last parameter, Ec, which is a measure of the relative importance of the conversion into heat of the energy of motion was assigned practical values.

The computation scheme will now be described: the values of T_i and $T_{\text{sat},\infty}$ were fixed, therefore fixing also p_{Vi} and $p_{\text{sat},\infty}$. The system total pressure P can then be calculated for each value of $W_{g\infty}$. Next, a trial value of $f'(\eta_\delta)$ is proposed. Using the conditions at the interface and the velocity solutions it can be shown that (ref. [6]):

$$\xi_V^2 = 240\{[f'(\eta_\delta)]^2[15R^2-12] + 4f'(\eta_\delta)+8\}^{-1}, \tag{17}$$

$$\eta_\delta = \tfrac{1}{2}Rf'(\eta_\delta)\xi_V, \tag{18}$$

and

$$g(0) = \tfrac{1}{2}Rf'(\eta_\delta)\eta_\delta. \tag{19}$$

As a result, ξ_V, η_δ and $g(0)$ are readily found and from the equation (15), the dimensionless concentration boundary-layer thickness ξ_d is calculated.

On the other hand the prescribed condition that the gas does not cross the interface into the liquid condensate can be written as

$$1-\frac{W_{g\infty}}{W_{gi}} = \tfrac{1}{4}Sc\,g(0)\xi_d \tag{20}$$

where $g(0)$ is known as above and W_{gi} is evaluated from equation (16) after some rearrangement:

$$W_{gi} = \frac{1-(p_{Vi}/P)}{1-(p_{Vi}/P)\left(1-\frac{M_V}{M_g}\right)}. \tag{21}$$

On returning to equation (20), ξ_d is numerically evaluated and its value compared with the previous result from equation (15). The computation is then either terminated or continued depending on whether the difference falls within a previously established degree of accuracy. If not, the original guess value of $f'(\eta_\delta)$ is replaced according to a policy to minimize the time for computations. The authors found the system of equations is little sensitive to changes in $f'(\eta_\delta)$.

When the computation is terminated, the resulting figures are introduced into either equation (11) or (12) to produce the corresponding value of ξ_T, at a given Ec. Finally, T_w is calculated through the condition f at the interface.

Heat transfer

The local heat flux q at the plate surface is that conducted across the layer of condensate. Using Fourier's law one arrives at

$$q = k_L(T_i - T_w)\sqrt{\frac{U}{v_L x}}\left(\frac{1}{\eta_\delta}\right). \tag{22}$$

The authors found convenient to present the results for heat transfer as ratios q/q^* and q/q^{**}, to bring to light the effects of viscous dissipation. In q, q^* and q^{**} the operating conditions are identical except that q includes superheating and energy dissipation, q^* refers to the case of saturated vapour and q^{**} is for no dissipation but with superheating. Therefore, q/q^* represents the excess of heat transferred to the wall above that for saturated vapour, this excess being the effects of both superheating plus viscous dissipation, whereas q/q^{**} highlights the effects of viscous dissipation only over those of superheating.

Thus, within the approximations of this work

$$\frac{q}{q^*} = \frac{T_i - T_w}{T_i^* - T_w}\cdot\frac{(1/\eta_\delta)}{(1/\eta_\delta^*)},$$

at a common $W_{g\infty}$, and

$$\frac{q}{q^{**}} = \frac{T_i - T_w}{T_i^{**} - T_w}\cdot\frac{(1/\eta_\delta)}{(1/\eta_\delta^{**})}$$

at common $W_{g\infty}$ and $T_\infty - T_{\text{sat},\infty}$. The variation of the liquid properties with temperature has been neglected.

For the problem of condensation of a pure vapour, $T_i = T_i^* = T_i^{**} = T_{\text{sat},\infty}$ and as a result of this the heat-transfer ratios are functions only of η_δ, η_δ^*, and η_δ^{**} [6].

RESULTS AND DISCUSSION

In the Table 1 of reference [1], the authors present a list of figures showing the relationship between $g(0)$ ($F(0)$ in that reference) and $1/\eta_\delta$. Those values could have been used in this research if it had not been for the little work added to the whole in programming

the solution to the set of algebraic equations, to obtain those quantities with the approximations of this present formulation and method of computation.

In a previous paper on the effect of viscous dissipation on the condensation rate of pure superheated steam, Saddy and Del Pozo [6] show in their Table 1 the results of the approximated method which are quite close to those arrived at by Minkowycz and Sparrow mentioned above.

The method of computation described earlier on begins with the especification of T_i, the saturation temperature at the interface. Thus, although the final results for $g(0)$ and η_δ are universal, the knowledge of the range of temperatures in between whose extremes T_i should lie is of primary importance to calculate those figures. Therefore the fluid system must be specified *a priori*. This is no disadvantage as compared with other methods of computation because the system has to be known beforehand when practical applications are to be made.

For steam as the condensing vapour and air as the non-condensable the following values of the parameters were used:

$Sc = 0{\cdot}55$
$T_{\text{sat},\infty} = 212°\text{F}$
$W_{g\infty} = 0{\cdot}0$, $0{\cdot}005$, $0{\cdot}02$, $0{\cdot}05$ and $0{\cdot}1$
$T_\infty - T_{\text{sat},\infty} = 0$, 100°F, 200°F and 400°F
$Ec = 0$, $0{\cdot}1$, $1{\cdot}0$ and $2{\cdot}0$.

The values of T_i were in the range from 170°F to $T_{\text{sat},\infty}$ and the fluids properties at those temperatures are the same used in reference [7].

Some of the results are listed in Tables 1 and 2 (complete list of tables with results and fluid properties are available on request). It is seen from Table 1 that at and above values of $g(0)$ about 6, $f'(\eta_\delta)$ is less than or equal to 0·04 which means that at low rates of condensation the streamwise velocity component at the interface can in fact be neglected. At the highest rates of condensation used in this work $f'(\eta_\delta)$ had its largest value at 0·088. Also, an increase in the rate of condensation obviously brings about an increase in the condensate layer thickness—$g(0)$ and η_δ are monotonic functions—as well as a decrease of the interface temperature T_i, at a fixed value of $W_{g\infty}$, caused by an accumulation of non-condensable there. This effect is more pronounced at large values of $W_{g\infty}$.

As it were expected on physical grounds, ξ_V and ξ_d diminish as $g(0)$ is augmented, because for forced convective flow it is well established that $\xi_V \sim (Re)^{-1/2}$ and $\xi_d \sim (Re\,Sc)^{-1/2}$, and also because with higher rates of condensation larger amounts of noncondensable concentrate at the interface and W_{gi} approaches $W_{g\infty}$ its value in the free stream.

Table 1. Results from the approximate solutions

T_i	$W_{g\infty}$	$g(0)$	η_δ	$f'(\eta_\delta)$	ξ_V	ξ_d
170	0·005	14·7718	2·0919	0·088	0·2700	0·4888
	0·02	7·1360	2·0346	0·044	0·5544	0·9902
	0·05	4·3000	1·9991	0·028	0·9038	1·5724
	0·10	2·8157	1·9566	0·019	1·3339	2·2256
180	0·005	13·7067	2·0841	0·082	0·2909	0·5262
	0·02	6·6126	2·0293	0·041	0·5973	1·0639
	0·05	3·9686	1·9961	0·025	0·9348	1·6219
	0·10	2·5811	1·9446	0·017	1·4398	2·3755
190	0·005	12·1409	2·0714	0·071	0·3281	0·5928
	0·02	5·8415	2·0203	0·036	0·6738	1·1940
	0·05	3·4798	1·9796	0·022	1·1014	1·8815
	0·10	2·2360	1·9220	0·015	1·6274	2·6309
200	0·005	9·6225	2·0507	0·055	0·4131	0·7436
	0·02	4·5920	2·0021	0·027	0·8492	1·4844
	0·05	2·6855	1·9489	0·017	1·3910	2·3069
	0·10	1·6789	1·8633	0·011	2·0448	3·1568
210	0·005	4·1031	1·9917	0·023	0·9448	1·6378
	0·02	1·7944	1·8777	0·011	1·9438	3·0346
	0·05	0·9255	1·6735	0·006	3·0069	4·1912
	0·10	0·5065	1·4066	0·004	3·8894	4·9839

Table 2. Results for ξ_T as function of $W_{g\infty}$ and Ec

T_i	Ec	$W_{g\infty}$ 0·005	0·02	0·05	0·10
170	0·0	0·2889	0·6017	0·9774	1·4549
	0·1	0·2733	0·5678	0·9223	1·3762
	1·0	0·1877	0·3802	0·6149	0·9218
	2·0	0·1446	0·2899	0·4674	0·6985
180	0·0	0·3055	0·6306	1·0376	1·5473
	0·1	0·2893	0·5949	0·9791	1·4643
	1·0	0·1981	0·3985	0·6533	0·9831
	2·0	0·1527	0·3045	0·4971	0·7456
190	0·0	0·3358	0·6941	1·1452	1·7118
	0·1	0·3137	0·6546	1·0810	1·6217
	1·0	0·2167	0·4382	0·7224	1·0933
	2·0	0·1670	0·3353	0·5505	0·8303
200	0·0	0·4067	0·8428	1·3973	2·0850
	0·1	0·3840	0·7945	1·3204	1·9810
	1·0	0·2603	0·5318	0·8861	1·3497
	2·0	0·2008	0·4077	0·6764	1·0261
210	0·0	0·8781	1·8369	2·9028	3·8267
	0·1	0·8275	1·7406	2·7771	3·6918
	1·0	0·5559	1·1804	1·9458	2·6978
	2·0	0·4284	0·9034	1·4809	2·0553

From Table 2 and for the same reason as above, as the condensation rate increases (i.e. T_i decreases), the thermal boundary-layer thickness decreases—$\xi_T \sim (Re\,Pr)^{-1/2}$, for all values of $W_{g\infty}$ and at a given Ec. This result is of particular importance in explaining the enhancement of heat flux at the solid surface: the resistance in the vapour–gas side to heat transfer to the wall is thereby decreased. Moreover this effect becomes slightly more marked as the parameter Ec becomes

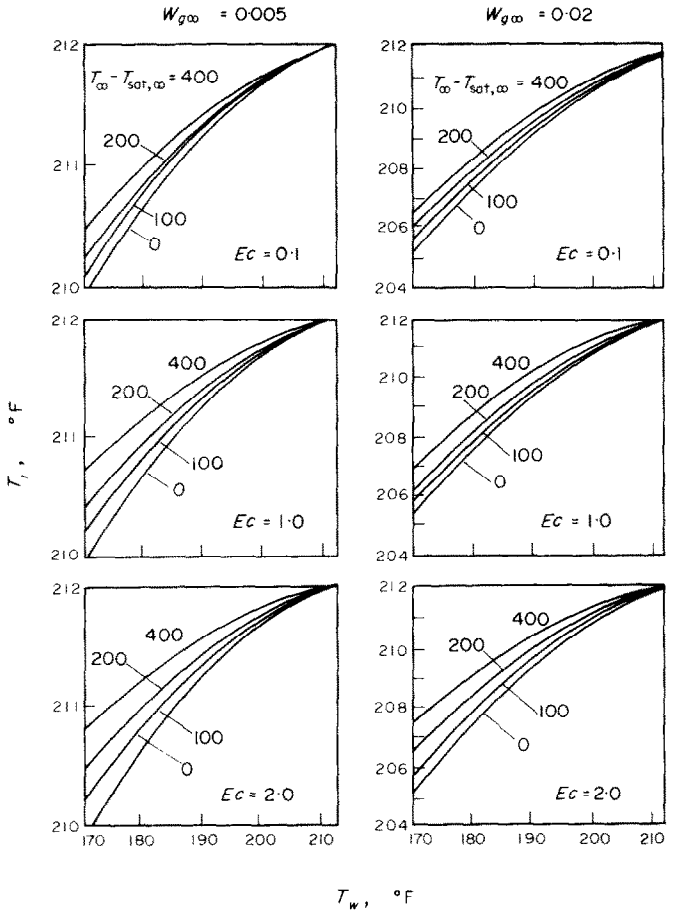

FIG. 2(a). Interface temperature as function of operating conditions: $W_{g\infty} = 0{\cdot}005$ and $0{\cdot}02$.

larger, which may be brought about by varying either or both of two independent operating variables: an increase in the free stream velocity U and a decrease in the noncondensable mass fraction in the free stream, $W_{g\infty}$.

Table 3. Typical results for W_{gi} as function of $W_{g\infty}$ and T_i

T_i	$W_{g\infty}$ / P	0·005 14·7419	0·02 14·8824	0·05 15·1769	0·10 15·7112
170		0·7013	0·7047	0·7114	0·7229
175		0·6578	0·6617	0·6696	0·6830
180		0·6076	0·6122	0·6215	0·6372
185		0·5495	0·5549	0·5658	0·5843
190		0·4820	0·4884	0·5013	0·5232
195		0·4029	0·4105	0·4260	0·4520
200		0·3097	0·3189	0·3375	0·3687
205		0·1980	0·2092	0·2317	0·2694
210		0·0658	0·0796	0·1071	0·1531
212		0·005	0·02	0·05	0·10

Finally, in Fig. 2 it is shown the variation of the interface saturation temperature T_i with the solid surface temperature T_w, for the several degrees of superheating and viscous dissipation analysed in this work, each set of three figures for a given gas mass fraction. The general trend is that as T_w approaches $T_{sat,\infty}$, T_i also gets closer to $T_{sat,\infty}$, whatever the values of the other parameters are. Some other conclusions can be drawn from Fig. 2: at a given value of T_w, increases in both $T_\infty - T_{sat,\infty}$ and Ec produce increases in T_i and consequently decreases in η_δ, whereas larger gas mass fractions $W_{g\infty}$ should lower T_i, which as a result causes an increase in η_δ.

All these results are most useful in calculating the heat-transfer ratios.

Results for heat transfer

The results for heat fluxes to the solid wall are presented in the Figs. 3 and 4, for q/q^* and q/q^{**}, respectively. As the temperature at the interface T_i is less

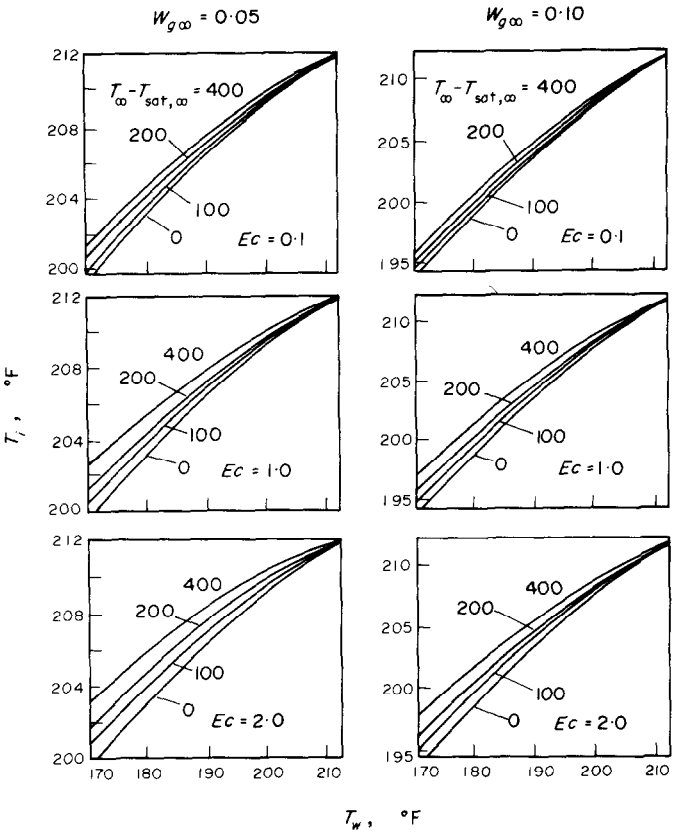

FIG. 2(b). Interface temperature as function of operating conditions: $W_{g\infty} = 0{\cdot}05$ and $0{\cdot}1$.

than $T_{sat,\infty}$ when the noncondensable is present, one could reason as follows: when superheating is also present, the amount of heat which reaches the interface comes from two mechanisms—by conduction through the gas–vapour thermal layer above it and also as latent heat of condensation; to maintain a given temperature difference $T_i - T_w$ in the two cases of saturated and superheated mixtures with noncondensable, all the other operating variables the same, the fraction of that amount as latent heat is less in the case of superheated than in the case of saturated mixtures, which produces a thinner layer of condensate in the former case. As the heat flux is inversely proportional to the dimensionless condensate layer, the ratio between the heat fluxes, in the presence of noncondensable, with superheating to saturated vapour is always greater than unity (a very good discussion of the curves is presented in [1] and [6]).

When viscous dissipation is considerable and must be taken into account, its effect is to heat up the layer of gas–vapour mixture on top of the condensate above its saturation temperature. When the vapour is already superheated, the dissipation into heat of the energy of motion will add to the existing degree of superheating both working in the same direction. Hence, the same reasoning as presented above applies and q/q^* and q/q^{**} are greater than unity.

From what has so far been described the two parameters $T_\infty - T_{sat,\infty}$ and Ec have the same qualitative effect over the heat flux to the wall. Both produce greater increase to the numerator than to the denominator of equations (23) and (24).

On the other hand, the effect of $W_{g\infty}$ on the heat flux on forced convection condensation is well known. It is clear that it produces greater negative variation to the denominator than to the numerator of equations (23) and (24). Therefore, q/q^* and q/q^{**} increase with larger amounts of noncondensable in the free stream.

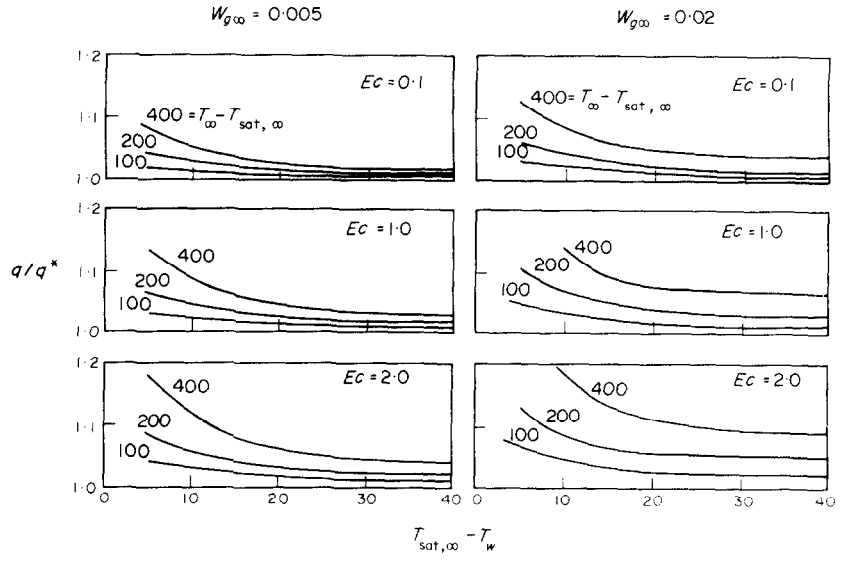

FIG. 3(a). Heat-transfer results, q/q^*. Effect of superheating plus viscous dissipation: $T_{sat,\infty} = 212°F$, $W_{g\infty} = 0{\cdot}005$ and $0{\cdot}02$.

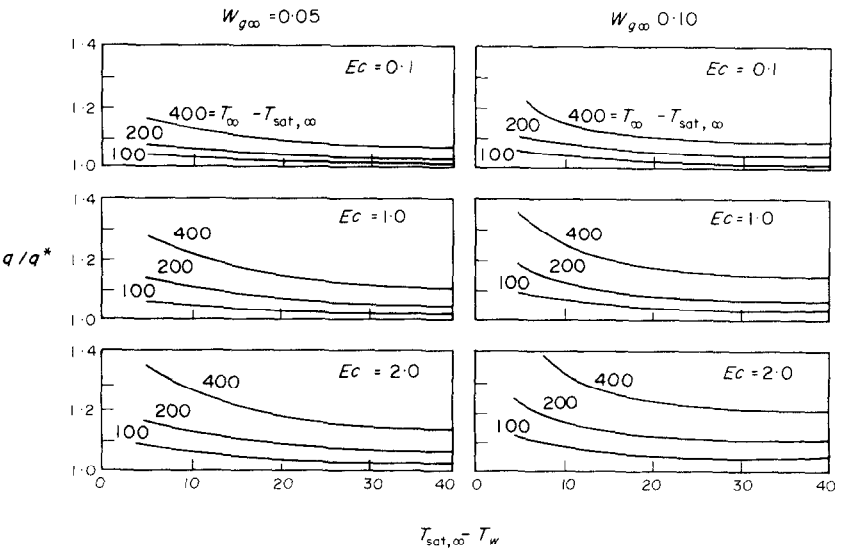

FIG. 3(b). Heat-transfer results, q/q^*. Effect of superheating plus viscous dissipation: $T_{sat,\infty} = 212°F$, $W_{g\infty} = 0{\cdot}05$ and $0{\cdot}1$.

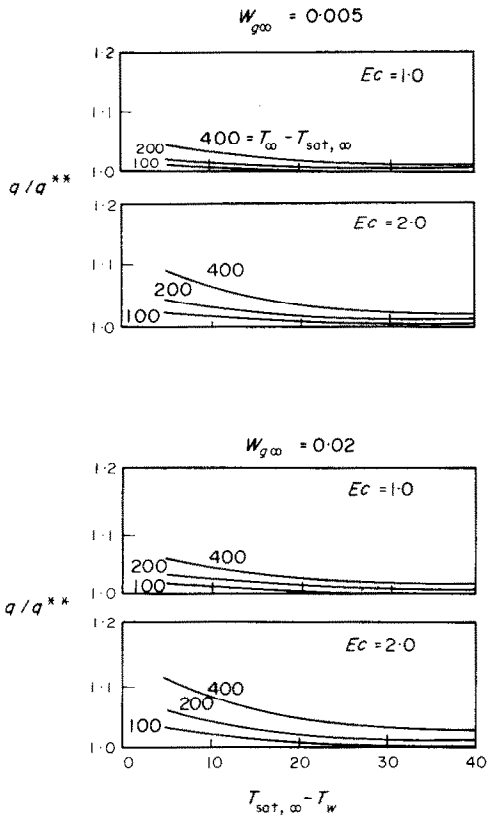

FIG. 4(a). Heat-transfer results, q/q^{**}. Effect of viscous dissipation over that of superheating: $T_{sat,\infty} = 212°F$, $W_{g\infty} = 0{\cdot}005$ and $0{\cdot}02$.

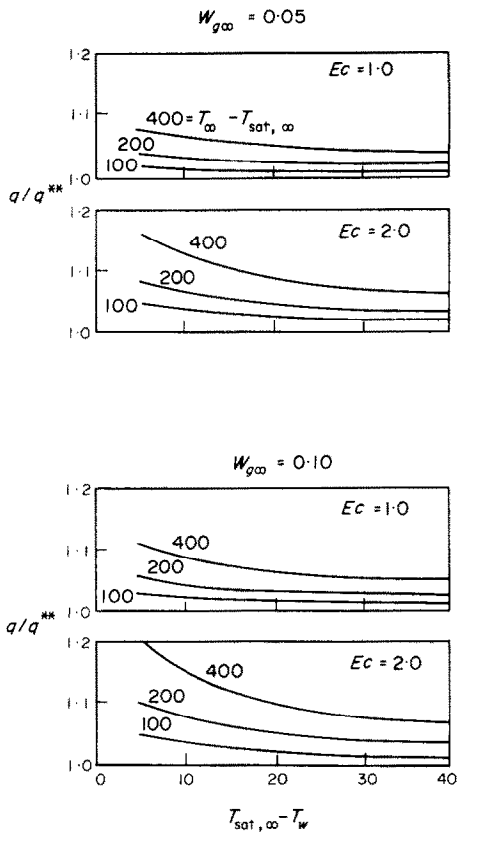

FIG. 4(b). Heat-transfer results, q/q^{**}. Effect of viscous dissipation over that of superheating: $T_{sat,\infty} = 212°F$, $W_{g\infty} = 0{\cdot}05$ and $0{\cdot}1$.

To highlight the effects of Ec on the heat flux ratios, Tables 4 and 5 were prepared to set out their percent increase as function of $W_{g\infty}$. For values of Ec equal to 0·0 and 0·1, the added effect of viscous dissipation is negligible; hence, increases in the heat flux are entirely because of the superheating. Appreciable enhancement is observed for the higher values of Ec and at high proportions of non-condensable, but never above 10 per cent.

For smaller values of $T_\infty - T_{sat,\infty}$ these effects are less pronounced and become not significant.

Although the results of this simple theory presented at excessively high Eckert numbers may not meet a direct application to the steam–air system of this example (the analysis of laminar boundary-layers might not apply any more because of the high free stream velocities), they are most useful however, in helping analysing the trends. These then can be applied to other systems.

Table 4. Values of $(q/q^{**} - 1) \times 100$
$T_\infty - T_{sat,\infty} = 400°F$
$T_{sat,\infty} - T_w = 20°F$

Ec	$W_{g\infty}$ 0	0·005	0·02	0·05	0·1
0·1	0·0	0·0	0·0	0·0	0·0
1·0	1·0	1·8	2·4	4·8	6·0
2·0	1·9	3·7	5·2	8·0	10·0

Table 5. Values of $(q/q^* - 1) \times 100$

$T_\infty - T_{sat,\infty} = 400°F$
$T_{sat,\infty} - T_w = 20°F$

Ec	$W_{g\infty}$ 0	0·005	0·02	0·05	0·1
0·0 and 0·1	1·8	2·4	5·4	8·0	10·8
1·0	2·8	4·2	7·8	13·8	17·8
2·0	5·3	6·0	10·0	17·7	24·0

CONCLUSIONS

On the grounds of a simple model based on forced condensation boundary-layer flow it is discussed in this work the mechanisms by which heat transfer to the solid wall, in the presence of noncondensable and superheating, can be enhanced by viscous dissipation in the gas–vapour-side.

The effect of viscous dissipation is to increase the temperature at the liquid–mixture interface thereby decreasing the thickness of the thermal boundary-layer set up on top of the condensate. This effect is very similar to that of superheating both causing an increase in the rate of heat transferred to the solid wall.

For all values of Ec studied herein, the significance of viscous dissipation to heat flux is practically unimportant at low values of $W_{g\infty}$ and $T_\infty - T_{\text{sat.}\infty}$.

REFERENCES

1. W. J. Minkowycz and E. M. Sparrow, The effect of superheating on condensation heat transfer in a forced convection boundary layer flow, *Int. J. Heat Mass Transfer* **12**, 147–154 (1969).
2. E. M. Sparrow, W. J. Minkowycz and M. Saddy, Forced convection condensation in the presence of noncondensable and interfacial resistance, *Int. J. Heat Mass Transfer* **10**, 1829–1845 (1967).
3. R. D. Cess, Laminar film condensation on a flat plate in the absence of a body force, *Z. Angew. Math. Phys.* **11**, 426–433 (1960).
4. J. C. Y. Koh, Film condensation in a forced convection boundary layer flow, *Int. J. Heat Mass Transfer* **5**, 941–954 (1962).
5. M. Schmal, Eine Näherungslösung für die Kondensation von Laminar strömendem Dampf mit beliebigen Druckgradienten bei kleiner Mach-Zahl und Konstanten Stöffwerten, Dissertation T.U. Berlin (1970).
6. M. Saddy and F. V. Del Pozo, Condensation heat transfer in forced convection flow with viscous dissipation, *Lat. Am. J. Chem. Engng Appl. Chem.* **2**(2), 89–102 (1972).
7. S. M. M. Ferreira, Condensação na Presença de Vapor Superaquecido e Resistência Interfacial, M.Sc. thesis, COPPE/UFRJ, Rio de Janeiro, Brazil (1967).

ACCROISSEMENT PAR LA DISSIPATION VISQUEUSE DU TRANSFERT THERMIQUE AVEC CONDENSATION EN PRESENCE D'UN GAZ INCONDENSABLE

Résumé—On propose un modèle simple basé sur l'écoulement forcé à couche limite avec condensation pour étudier les mécanismes de transfert de chaleur à partir d'un paroi solide, en présence d'un gaz incondensable avec surchauffe et dissipation visqueuse dans la phase gaz–vapeur.

On obtient des résultats numériques pour le système vapeur d'eau–air, à une température de saturation égale à 100 °C, pour quelques degrés de surchauffe et quelques fractions en masse d'incondensable qui correspondent à des applications pratiques.

On montre qu'à travers un accroissement de température à l'interface condensat-vapeur–gaz, l'effet de la dissipation visqueuse est de diminuer l'épaisseur de la couche limite thermique au dessus du condensat, dans la phase gazeuse, effet comparable à celui de la surchauffe. Ces deux effets causent un accroissement du flux thermique à la paroi.

DIE ERHÖHUNG DES WÄRMEÜBERGANGS BEI DER KONDENSATION INERTGASHALTIGER DÄMPFE DURCH DISSIPATION

Zusammenfassung—Es wird ein einfaches Modell zur Untersuchung des Wärmeübergangs an eine feste Wand unter Berücksichtigung der Anwesenheit nichtkondensierbarer Gase, der Überhitzung und der Dissipation im Dampf-Gas-Gemisch vorgeschlagen, das auf dem Grenzschichtmodell für Kondensation bei erzwungener Konvektion basiert.

Die Rechnung wird für das System Wasserdampf-Luft bei einer Sättigungstemperatur von 100°C durchgeführt für verschiedene Überhitzungen und in der Praxis vorkommende Inertgasanteile. Es wird gezeigt, daß die Dissipation durch die Erhöhung der Phasengrenzflächentemperatur, ähnlich wie die Überhitzung, zu einer Verringerung der gemischseitigen thermischen Grenzschichtdicke führt. Beide Effekte bewirken eine Zunahme des Wärmestroms an die Wand.

ИНТЕНСИФИКАЦИЯ ТЕПЛООБМЕНА ЗА СЧЕТ ВЯЗКОЙ ДИССИПАЦИИ В СЛУЧАЕ КОНДЕНСАЦИИ ПРИ НАЛИЧИИ НЕКОНДЕНСИРУЮЩИХСЯ ЧАСТИЦ МАССЫ

Аннотация — Для изучения механизмов переноса тепла к твердой стенке при наличии неконденсирующихся частиц массы и перегрева, сопровождаемого вязкой диссипацией со стороны газ-пар, предложена простая модель, основанная на течении пограничного слоя при вынужденной конвекции и конденсации.

Получены численные результаты для системы пар-воздух при температуре насыщения 212°F, перегреве в несколько градусов и при наличии неконденсирующихся частиц массы, пригодные для практического использования.

Показано, что как и в случае перегрева, толщина теплового пограничного слоя над конденсатом уменьшается за счет вязкой диссипации при увеличении температуры на поверхности раздела конденсат-газ-пар. Тепловой поток на стенке увеличивается как за счет перегрева, так и вязкой диссипации.